

Fabrication of Silica Nanoparticles with Both Efficient Fluorescence and Strong Magnetization, and Exploration of Their Biological Applications

Faisal Mahtab, Yong Yu, Jacky W. Y. Lam, Jianzhao Liu, Bei Zhang, Ping Lu, Xixiang Zhang, and Ben Zhong Tang*

Nanoparticles with both efficient light emission and strong magnetization (MFSNPs) are fabricated by one-pot, surfactant-free sol–gel reaction of tetraethoxysilane and silole-functionalized siloxane in the presence of citrate-coated magnetite nanoparticles. The MFSNPs are uniformly sized with smooth surfaces. They possess core–shell structures and exhibit appreciable surface charges and hence good colloidal stability. The MFSNPs are superparamagnetic, exhibiting no hysteresis at room temperature. UV irradiation of the suspension of MFSNPs in ethanol gives strong green emission at 486 nm, thanks to the novel aggregation-induced emission characteristics of the silole aggregates in the hybrid nanoparticles. The MFSNPs can selectively stain the cytoplasmic regions of the living cells. Addition of (3-aminopropyl)triethoxysilane during the fabrication of MFSNPs has generated MFSNP-NH₂ with numerous amino groups decorated on the surface, enabling the nanoparticles to immobilize bovine serum albumin efficiently.

1. Introduction

Nanoparticles with both efficient fluorescence and strong magnetization may find high-technological applications in ultrasensitive assays, living cell labeling, biological separation, site-specific drug delivery, magnetic resonance imaging, and magnetocytosis.^[1] Little effort has, however, been devoted to the development of such nanoparticles, in comparison to the great wealth of the studies on the particles with a single attribute of either fluorescence or magnetization.^[2–17]

Silica and polymer are favorable host materials for the inclusion of chromophores and nanoclusters because of their optical

transparency and biological compatibility. The encapsulation can protect the dye molecules from external perturbations such as oxygen and ions dissolved in solutions. For magnetic nanoclusters, the encapsulation can prevent them from agglomerating into large chunks. The silica/polymer matrix also provides a useful platform for surface chemistry, enabling the nanoparticle surfaces to be chemically modified for further functionalization.

Many commercially available organic dyes, such as rhodamine, ethidium bromide, and Nile Red, emit efficiently in the dilute solutions but become weakly fluorescent or even nonemissive when aggregated in the solid state.^[18–23] This phenomenon is very common and has been attributed to the nonradiative decay

of sandwich-shaped excimers and exciplexes formed among the closely packed dye molecules in the aggregates. A low dye loading in the particle may be free of aggregation but can only offer weak emission. The light emission cannot be enhanced by putting more dye molecules into a particle because of the notorious effect of aggregation-caused quenching (ACQ). Various chemical, physical, and engineering approaches and processes have been developed to mitigate the ACQ effect. The attempts have, however, met with only limited success.^[24–26] Such problems can be avoided by the use of semiconductor quantum dots (e.g., CdSe). However, quantum dots generally show small Stokes shifts (hence heavy self-absorption) and low fluorescence quantum yields, in addition to their high toxicity.^[27–30] Many research groups have incorporated magnetic nanoclusters into the nanoparticles but the magnetizations of the clusters are commonly low, which greatly limit the scope of their potential applications.^[31–34]

We have worked on the development of luminescent materials with efficient light emissions in the solid state and observed a novel phenomenon of aggregation-induced emission (AIE): a group of nonemissive, propeller-like molecules are induced to emit efficiently by aggregate formation.^[35–39] The AIE effect can boost the fluorescence quantum yields (Φ_F 's) of the molecules by up to two orders of magnitude. Taking advantage of such effects, we have utilized the AIE dyes for the fabrication of highly emissive fluorescent silica nanoparticles (FSNPs) with core–shell structures.^[40] The FSNPs pose

Dr. F. Mahtab, Y. Yu, Dr. J. W. Y. Lam, Dr. J. Liu, Dr. P. Lu, Prof. B. Z. Tang
Department of Chemistry
The Hong Kong University of Science & Technology
Clear Water Bay, Kowloon, Hong Kong, China
Fax: +852–2358–1594
E-mail: tangbenz@ust.hk

Prof. B. Z. Tang
Department of Polymer Science and Engineering
Zhejiang University
Hangzhou 310027, China

Prof. B. Zhang, Prof. X. Zhang
Department of Physics
The Hong Kong University of Science & Technology
Clear Water Bay, Kowloon, Hong Kong, China

DOI: 10.1002/adfm.201002572

no toxicity to living cells and can function as fluorescent visualizers for intracellular imaging. We have also worked on the fabrication of nanocomposites of superparamagnetic iron and its oxides and silicides with high magnetizations and zero hysteresis losses by the reaction of iron salts in aqueous ammonia and by the pyrolysis of organoiron polymers at high temperatures.^[41–45] Starting from cobalt–polymer complexes, we have recently succeeded in the preparation of soft ferromagnetic cobalt nanoclusters, whose magnetizations are very high (saturation magnetization (M_s) up to ~ 118 emu g^{−1}) and coercivities are very low (H_c down to ~ 0.045 KOe). The encouraging results described above prompt us to explore the possibility of synthesizing magnetic fluorescent silica nanoparticles (MFSNPs) with core–shell structures, in an effort to prepare nanostructured materials that show high fluorescence efficiency and magnetic susceptibility. In this paper, we show how these goals have been achieved and demonstrate the biological applications of the synthesized MFSNPs.

2. Results and Discussions

2.1. Fabrication of MNPs and MFSNPs

We first prepared magnetic clusters as seeds for the fabrication of MFSNPs. Among various materials, we chosen magnetite (Fe_3O_4) because of its biocompatibility and potential applications in biology and medicine such as enzyme and protein immobilization, magnetic resonance imaging, RNA and DNA purification, etc.^[46–48] The magnetite nanoparticles (MNPs) were prepared following the literature method, which was based on the chemical coprecipitation of Fe^{2+} and Fe^{3+} ions by adding an aqueous ammonium hydroxide solution (1.5 M) into a mixture of iron(II) and iron(III) chlorides with a molar ratio of 1:1. However, for ultrafine magnetic particles, the large surface to volume ratios and the magnetic dipole–dipole attractions between the particles generally result in agglomeration.^[49–51] Thus, in the last step of reaction, the MNPs are coated by stabilizer molecules of trisodium citrate to enhance their dispersion and stability in the solutions (Scheme 1). The resultant citrate-modified MNPs (MNP-C) were precipitated in acetone, washed with deionized water, and dried under vacuum. Their

morphologies are investigated by transmission electron microscopy (TEM). As shown in Figure S1, all the MNP-C are spherical in shape and monodispersed with diameters of 9.80 ± 2.36 nm. Their electron diffraction pattern shows rings corresponding to hkl values of {220}, {311}, {400}, {440}, and {511} of magnetite crystals with cubic inverse spinal structure.^[52] Zeta potential analysis reveals that the MNP-C posses high surface charge and hence excellent colloidal stability.

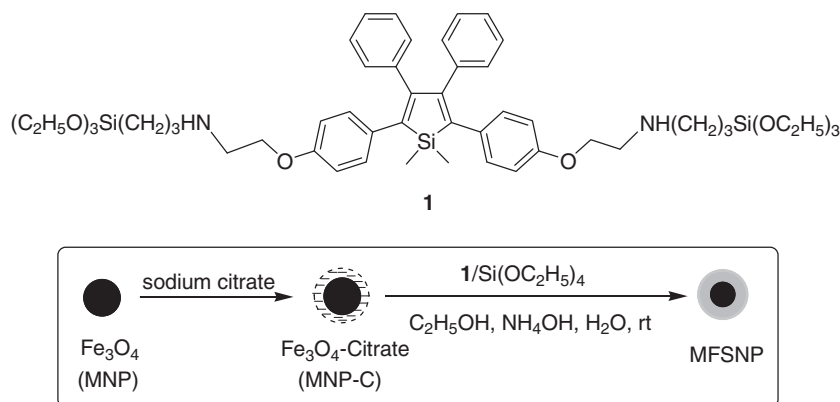
After the success of preparing MNP-C, we then worked on the synthesis of AIE luminogen. We prepared the silole derivative and covalently linked it to (3-aminopropyl)triethoxysilane (APS) according to our previous paper.^[40] The silole-APS adduct gives an $(M + 1)^+$ peak at 940.4962 in its high resolution mass spectrum (Figure S2 in the Supporting Information), confirming the formation of expected product 1. Compound 1 is then mixed with tetraethoxysilane (TEOS) and their sol–gel reaction is catalyzed by ammonium hydroxide in an aqueous mixture of MNP-C for 24 h, which furnishes MFSNPs with magnetic cores coated with luminogen-containing silica shell. The surfaces of the MFSNPs can be readily modified by adding other siloxanes into the reaction mixture. For example, MFSNP- NH_2 , can be readily synthesized in the presence of APS, by which their surfaces are coated with numerous amino functionalities.

2.2. Reaction Optimization

The size and morphology of the MFSNPs are affected by many parameters. As reported in the previous studies, the sizes of the MFSNPs become smaller with an increase in the amount of magnetite added. The thickness of the silica shell, on the other hand, can be controlled by the TEOS concentration.^[53,54] We also studied the effects of MNP-C, TEOS, and NH_4OH concentrations on the sol–gel reactions. Under the conditions shown in Table S1, row 1, discrete, uniform nanoparticles are formed in MFSNP-1 (Figure S3). However, lowering the TEOS concentration has decreased the thickness of the silica shell and hence the size of the resultant MFSNP-2. The particles of MFSNP-2 are aggregated because not all the triethoxysilyl groups of 1 are hydrolyzed and remain on the particle surface. The particles of MFSNP-3 are smaller than MFSNP-1 but larger than those of MFSNP-4 as the amount of MNP-C used for the sol–gel reaction

is in between those for the fabrication of MFSNP-1 and MFSNP-4. Ammonium hydroxide plays an important role in the sol–gel process. The hydrolysis of TEOS and 1 becomes slower in the presence of small amounts of NH_4OH , which leads to the particle aggregation and promotes the formation of FSNPs (Figure S3E). The particles of MFSNP-6 are also clustered together, probably due to the insufficient amount of TEOS in the reaction mixture, which cannot coat and encapsulate all the particles of MNP-C and 1.

The addition mode of TEOS and 1 strongly affects the morphology and properties of the synthesized MFSNPs. If 1 is added to the MNP-C solution prior to TEOS, it will



Scheme 1. Chemical structure of silole-APS adduct 1 and the synthetic route to magnetic fluorescent silica nanoparticles.

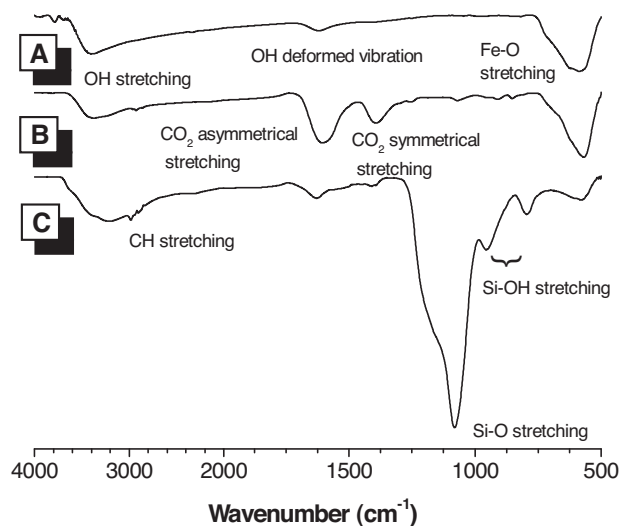


Figure 1. IR spectra of A) MNPs, B) MNP-C, and C) MFSNPs (sample taken from Table S1, no. 4).

produce aggregates of MFSNP-7 (Figure S4). The resultant particles contain the expected carbon, oxygen, iron, and silicon elements (Figure S5) but are nonluminescent because of the close proximity of the fluorophors to the metallic species. Therefore, the two reactants are either added simultaneously or their mixture is used in order to obtain fluorescent MFSNPs.

2.3. Structural Characterization

We first characterized the MFSNPs by IR spectroscopy. **Figure 1** shows the IR spectrum of MFSNPs; for comparison, the spectra of MNPs and MNP-C are also given in the same figure. The MNPs show O–H stretching, O–H deformed, and Fe–O stretching vibrations at 3408, 1633, and 584 cm^{-1} , respectively. After surface coating, the first two peaks are intensified due to their overlapping with the O–H and CO_2 asymmetrical stretchings of the citrate ions. A new peak associated with CO_2 symmetrical stretching is also observed at 1381 cm^{-1} . All these suggest the success of the formation of MNP-C.

After sol-gel reaction with **1** and TEOS, the peak intensity at $\sim 3300 \text{ cm}^{-1}$ is further enhanced. Weak absorptions assigned to C–H stretching vibration of **1** are observed at 2980 and 2870 cm^{-1} in MFSNPs. Absorption peaks associated with Si–O and Si–OH stretching vibrations are also emerged at 1081, 951, and 751 cm^{-1} , revealing that **1** and TEOS are covalently bonded on the MNP-C surface through silanization with the OH groups. TEM analysis show that MFSNPs, similar to MNP-C, are monodispersed with magnetic cores (mean diameter = $19.15 \pm 6.35 \text{ nm}$) surrounded by silica shell with thickness of $27.98 \pm 2.06 \text{ nm}$ (**Figure 2**).

Estimation by energy dispersive X-ray spectroscopy (EDX) depicts that the MFSNPs contain Fe, Si, O, N, and C elements (**Figure 3**). In contrast, no nitrogen and silicon atoms are detected in MNP-C (**Table 1**). X-ray photoelectron spectroscopy (XPS) analysis reveals that MFSNPs contain the expected silicon and nitrogen atoms (**Figure 4A**). The surfaces of the MFSNPs

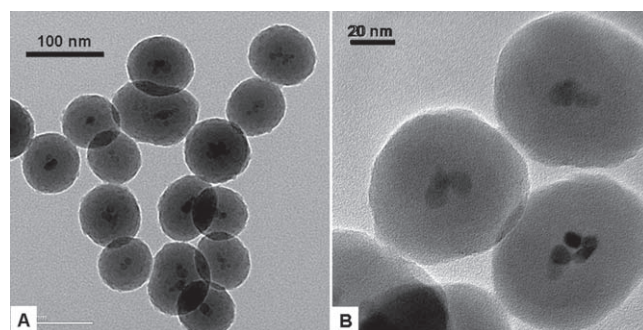


Figure 2. TEM images of MFSNPs (sample taken from Table S1, no. 4) at different magnifications.

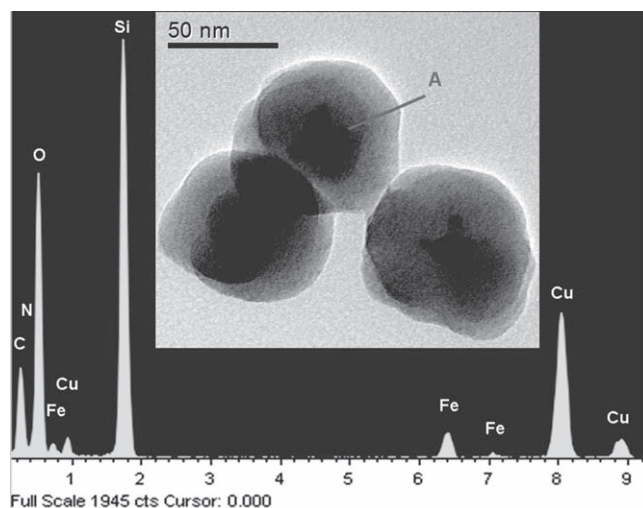


Figure 3. EDX spectrum of MFSNPs (sample taken from Table S1, no. 4). Inset: TEM image of the analysis site.

are mainly comprised of oxygen (57%) with small amounts of carbon (14.41%) and nitrogen (1.16%). A considerable amount of silicon (26.98%) is detected on the surface (**Table 1**). No iron species are found, revealing that MNP-C are mainly confined in the interior of the MFSNPs. Similarly, the XPS spectrum of MNP-C gives no peaks corresponding to $\text{Si}2s$ and $\text{Si}2p$ species at 154 and 101 eV, respectively, but displays $\text{Fe}2p_{3/2}$ peaks at 712 and 725 eV, which are in agreement with the oxidation

Table 1. Chemical compositions of the nanoparticles determined by EDX and XPS analyses^a.

Nanoparticle	Carbon	Nitrogen	Oxygen	Silicon	Iron
EDX					
MNP-C	50.99		7.75		41.26
MFSNPs	10.56	0.49	31.84	45.77	11.34
XPS					
MNP-C	4.95	0.44	52.39		41.95
MFSNPs	14.41	1.96	56.65	26.98	
MFSNP-NH ₂	11.90	5.58	50.11	24.40	
MFSNP-BSA	21.58	6.68	45.74	17.18	

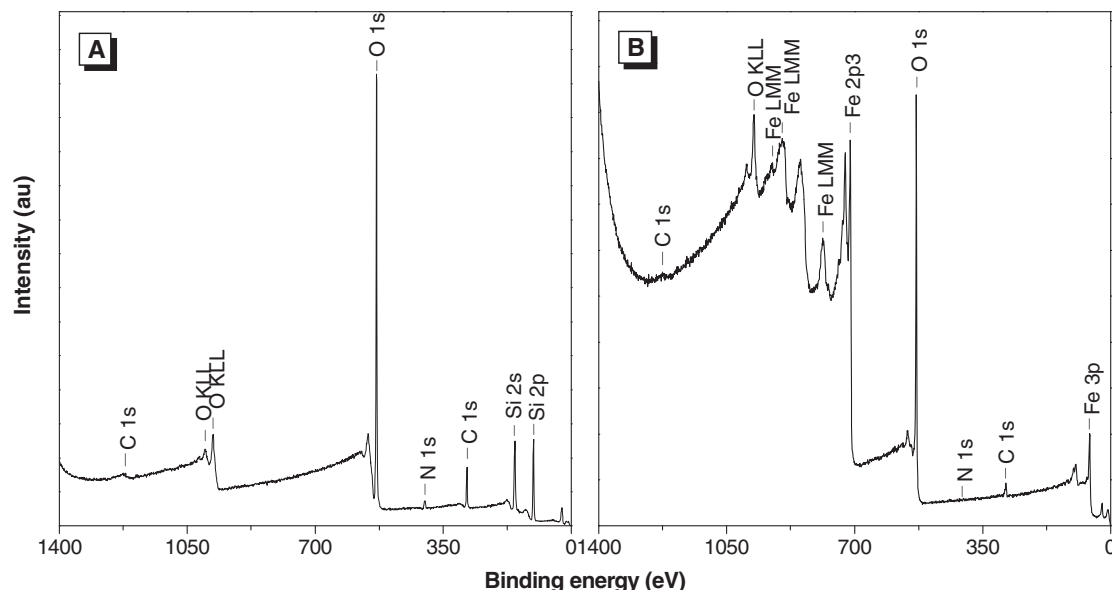


Figure 4. XPS spectra of A) MFSNPs (sample taken from Table S1, no. 4) and B) MNP-C.

state of Fe in Fe_3O_4 (Figure 4B).^[55] Like MFSNPs, the particles of MFSNP- NH_2 are uniform with expected compositions on the surface (Figure S6 and Figure S7A).

2.4. Colloidal Stability

Zeta potential analyses reveal that the MFSNPs, similar to MNP-C and MSNPs (prepared by sol-gel reaction of TEOS with MNP-C under similar conditions to those of MFSNPs), possess appreciable surface charges and hence good colloidal stability.^[56] The ζ potentials of MNP-C and MSNPs are negatively signed in almost the whole pH range, whose absolute magnitudes increase with increasing the pH value (Figure 5). At high pH or in the basic medium with high basicity, the acidic hydroxyl groups on the surfaces of MNP-C and MSNPs are converted into basic form, thus imparting them high negative charges.

The MFSNPs and MFSNP- NH_2 , however, exhibit positively signed ζ potentials at low pH due to the protonation of the amino groups contributed from **1** and the APS moieties.^[57,58] This event is less likely to occur at high pH but the dissociation of the hydroxyl groups is favored. This explains why the zeta potentials of MFSNPs and MFSNP- NH_2 are changed to negative sign and become higher with an increase in pH or the basicity of the aqueous medium. It is noteworthy that the ζ potential of MFSNP- NH_2 is still positively signed even at pH = 9 due to the relatively higher concentration of amino functionality on the particle surface. Thus, MFSNP- NH_2 may interact with negatively charged biomacromolecules at neutral pH. Indeed, addition of MFSNP- NH_2 to a buffer solution of bovine serum albumin (BSA) forms MFSNP-BSA, in which the nanoparticles dock on the BSA surface via noncovalent interactions such as electrostatic attraction and hydrophobic effect. The XPS spectrum of MFSNP-BSA is resembled to that of MFSNP- NH_2 (Figure S7B) but the C1s peak is much stronger due to the fine

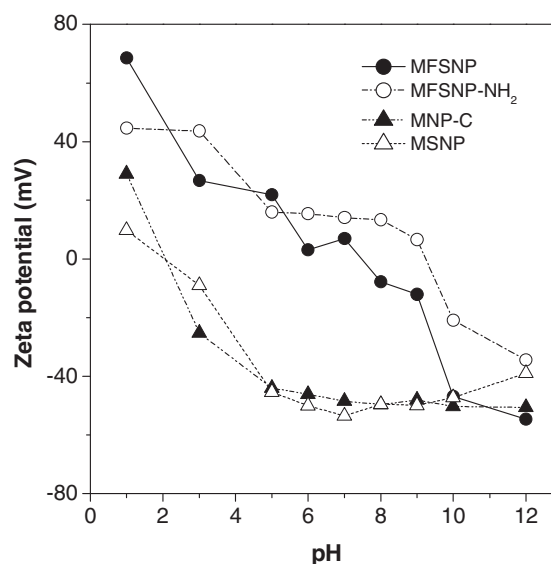


Figure 5. Zeta potentials of MNP-C, MSNPs, MFSNPs, (sample taken from Table S1, no. 4) and MFSNP- NH_2 in the aqueous media with different pH at room temperature.

contribution from the BSA (Table 1). The zeta potential changes from positive to negative sign at pH = 7, further providing evidence for the formation of MFSNP-BSA (Figure S8).

2.5. Magnetism

Since MNP-C and MFSNPs contain nanoscopic iron species, they are expected to be magnetically susceptible. Figure 6 shows the magnetization curves of the nanoparticles. With an increase in the magnetic field strength, the magnetization of MNP-C swiftly increases and ultimately reaches a saturation

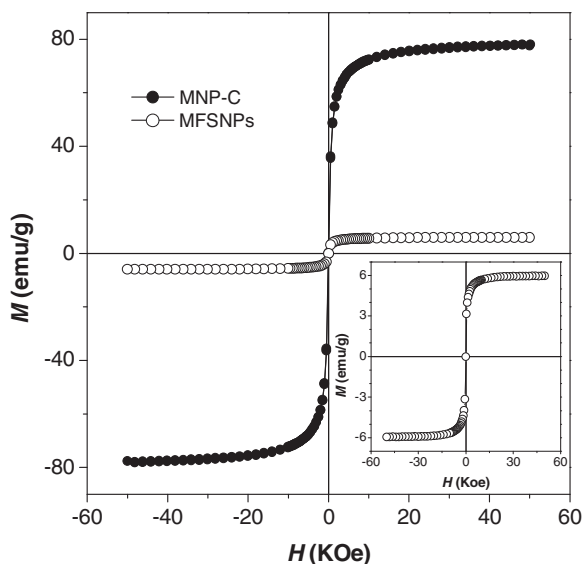


Figure 6. Plots of magnetization (M) versus applied magnetic field (H) at 300 K for MNP-C and MFSNPs (sample taken from Table S1, no. 4). Inset: rescaled spectrum of MFSNPs.

magnetization (M_s) of 78 emu g^{-1} . There is no hysteresis and both remanence and coercivity are zero, consistent with the superparamagnetic behaviors of the particles with nanoscale dimension.^[59] The magnetization curve of MFSNPs is similar to MNP-C. Although the M_s value (6 emu g^{-1}) is much lower than MNP-C, it is already superior to those particles prepared previously with M_s values in the range from 10^{-6} to 1 emu g^{-1} .^[30] The low magnetization of MFSNPs is, in some sense, understandable because the magnetite nanoparticles are covered by a thick silica shell, which has significantly diminished the inductive effect of the magnetic field.^[60]

2.6. Light Emission

Figure 7 shows the photoluminescence (PL) spectra of suspensions of MNP-C and MFSNPs in ethanol solutions. Nearly no fluorescence signals are recorded when MNP-C are photoexcited. Strong PL is, however, recorded at 486 nm in MFSNPs under the same measurement conditions. It is noteworthy that **1** is nonemissive in ethanol because the active intramolecular rotations of its phenyl blades have effectively annihilated the excited states, thus rendering the molecule nonluminescent. When **1** is covalently incorporated into and aggregated in the rigid silica network, its intramolecular rotations are restricted, which blocks the nonradiative relaxation channels and populates the radiative decay, thus making the MFSNPs emissive.^[35–39] The fluorescence quantum yield of MFSNPs measured by integrating sphere is reasonably high (7.11%), taking into the account that a low luminogen loading is used for the particle fabrication and the presence of iron species in MFSNPs. The light emission is very stable, with no change in the spectrum detectable after the MFSNPs have been put on shelves for several months without protection from light and air.

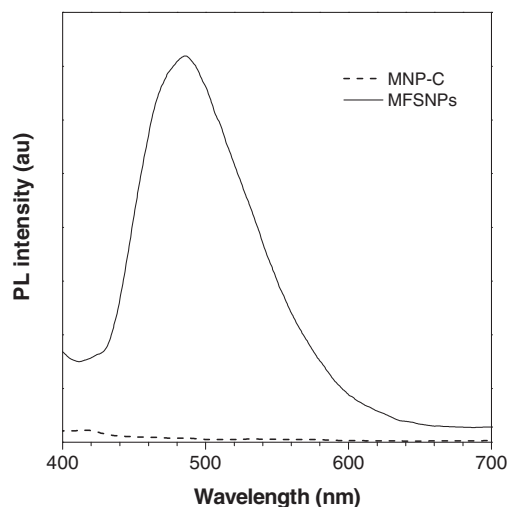


Figure 7. PL spectra of MNP-C and MFSNPs (sample taken from Table S1, no. 4) in ethanol solutions. Concentration: $100 \mu\text{g mL}^{-1}$; excitation wavelength: 370 nm.

The photographs in **Figure 8** show that both MNP-C and MFSNPs exhibit good dispersion in the solutions and can be attracted by a bar magnet. Although the solution of MNP-C

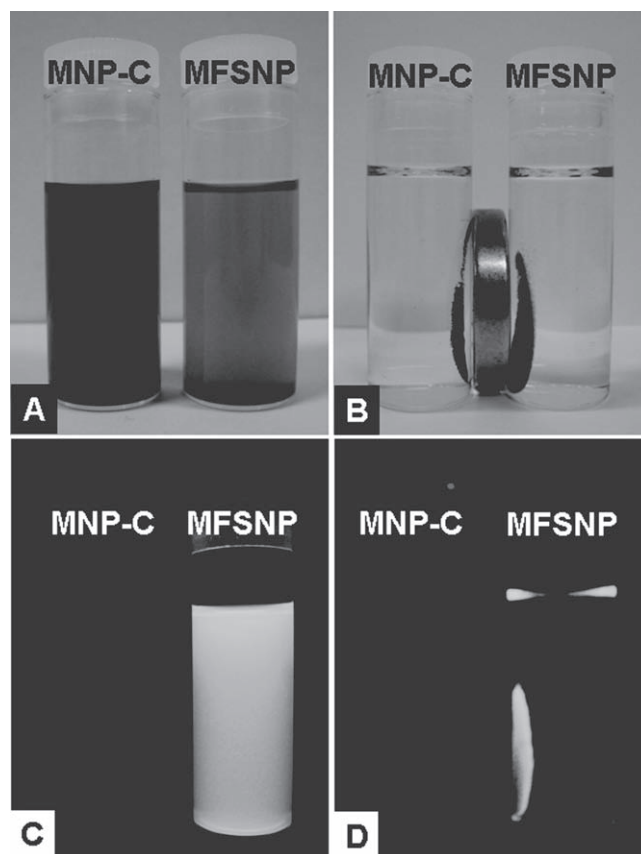


Figure 8. Photographs of ethanol solutions of A–B) MNP-C and MFSNPs (sample taken from Table S1, no. 4) taken under A–B) normal room lighting and C–D) UV illumination in the absence (A and C) and presence (B and D) of external magnetic field from a bar magnet.

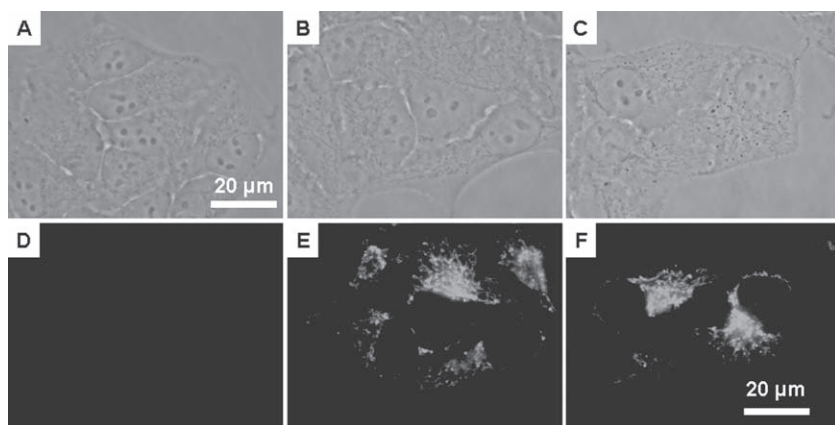


Figure 9. A–C) Bright-field and D–F) fluorescence images of HeLa cells before (A and D) and after labelling with MFSNPs (B and E) (sample taken from Table S1, no. 4) and MFSNP-NH₂ (C and F).

emits no light upon UV irradiation, strong green PL is observed in MFSNPs.

2.7. Cell Imaging

Previous studies show that the FSNPs can selectively stain the cytoplasmic regions of the living cells. Could MFSNPs and MFSNP-NH₂ also be utilized for such application? The answer is firmly “yes”, as shown by the images shown in **Figure 9**. Since the untreated HeLa cells emit no fluorescence upon UV irradiation (Figure 9D), the bright green emissions observed in Figures 9E and 9F clearly originate from MFSNPs and MFSNP-NH₂. The major route for the nanoparticles to enter the HeLa cells is through endocytosis and such a process is facilitated by high positive surface charges due to the electrostatic attraction with the anionic cell membrane (the zeta potential of HeLa cell membrane is reported to be -50 mV).^[61] This is experimentally proved by flow cytometry, which can determine the number of nanoparticles uptake by the cells. Due to the contribution from the amino groups on the surface, MFSNPs and MFSNP-NH₂ exhibit reasonably high positive charges at pH = 7, which may assist their uptake by the HeLa cells. The nanoparticles are then enclosed by the cell membrane to form small vesicles, which are then internalized by the cells. The nanoparticles are further processed in endosomes and lysosomes and are eventually released into the cytoplasm.^[50,62,63] When bound to the biomolecules, the nanoparticles may emit more intensely because the intramolecular rotations of the luminogens on the particle surface are further restricted. To confirm this, we prepared BSA solutions in PBS with various concentrations. After incubated with $500 \mu\text{g mL}^{-1}$ MFSNPs for 4 h at room temperature, the emissions of the solutions are investigated. As depicted in Figure S9, the fluorescence intensity increases with an increase in the BSA concentration and is saturated at high protein concentrations. Although the silica shell is hydrophilic, no MFSNPs are found in the nucleus; their sizes are probably still too big to pass through the nuclear membrane.

2.8. Protein Immobilization

Since MFSNP-NH₂ are magnetic and possess high positive charge, we can make use of such properties to determine their capability to hold BSA molecules. A series of BSA solutions in PBS with known concentrations are prepared. Same amount of MFSNP-NH₂ is then added to each solution. After incubation at room temperature for 1 h, the particles of the formed MFSNP-BSA are separated by a bar magnet. The MFSNP-BSA are washed with PBS and water, and dispersed in PBS. A calibration curve of absorbance versus BSA concentration is established (Figure S10) and the amount of BSA in MFSNP-BSA are determined from its absorbance. For 5 mg of MFSNP-NH₂, it can adsorb $274 \mu\text{g}$ of BSA. Thus, MFSNP-

NH₂ can be used as protein carrier or reactant for separating pure proteins from lysates.

3. Conclusion

In this work, we succeeded in synthesizing silica nanoparticles with both efficient fluorescence and strong magnetization by one-pot, surfactant-free sol-gel reaction of TEOS and **1** in the presence of MNP-C. The structure, morphology, and property of the MFSNPs are characterized and investigated by IR, TEM, EDX, XPS, zeta potential, fluorescence, and SQUID analyses. The MFSNPs are monodispersed with smooth surfaces. They possess core-shell structures and high positive surface charges at neutral pH and hence enjoy good colloidal stability. They are magnetically susceptible with zero remanence and coercivity, suggesting that they are good superparamagnets with high magnetization. Upon photoexcitation, the MFSNPs emit strong green light with fluorescence quantum yield of 7.11%, thanks to the AIE attribute of **1**. The MFSNPs can function as selective cell imaging bioprobes. Their surfaces can be readily modulated by varying the reactants. Addition of APS during the particle fabrication generates MFSNP-NH₂, which can serve as a protein carrier. We are currently working on the applications of our MFSNPs for cell specificity, biomedical imaging, cell separation, and bioassays. Details will be published in separate paper.

4. Experimental Section

Materials: Tetraethoxysilane (TEOS), dimethylsulfoxide (DMSO), (3-aminopropyl)triethoxysilane (APS), ferric chloride ($\text{FeCl}_3 \cdot 6\text{H}_2\text{O}$), ferrous chloride ($\text{FeCl}_2 \cdot 4\text{H}_2\text{O}$), and other reagents were all purchased from Aldrich and used as received. Silole-APS adduct (**1**) was prepared according to our previous publication.^[40]

Instrumentation: High-resolution mass spectra were recorded on a Finnigan TSQ 7000 triple quadrupole spectrometer operating in a MALDI-TOF mode. The morphologies and the electron diffraction patterns of the magnetite and magnetic fluorescent silica nanoparticles were investigated using JOEL 2010 transmission electron microscope

(TEM) at an accelerating voltage of 200 kV. Samples were prepared by drop-casting dilute dispersions onto copper 400-mesh carrier grids covered with carbon-coated formvar films. The solvent was evaporated in open air at room temperature. The size and thickness of the metal core and the silica shell were measured using TEM software (Digital Micrograph 365 Demo). The diameters of the magnetic core at different directions were measured and the mean value was reported. Photoluminescence spectra were recorded on a Perkin-Elmer LS 50B spectrofluorometer with a Xenon discharge lamp excitation. The zeta potentials of the nanoparticles (0.05 mg mL^{-1}) were determined in water at room temperature using a ZetaPlus Potential Analyzer (Brookhaven instruments corporation, USA). The pH of the suspensions was adjusted by adding hydrochloric acid and ammonium hydroxide solutions. Magnetization of the nanoparticles was measured using a superconducting quantum interference device magnetometer (Quantum Design MPMS-JS).

Particle Fabrication: 1) Synthesis of citrate-modified magnetite nanoparticles: Citrate-modified magnetite nanoparticles (MNP-C) were prepared by chemical coprecipitation of iron salts in basic medium followed by surface coating of the resultant magnetite nanoparticles by citrate ions. The precipitation was carried out in aqueous medium containing equal molar ratio of Fe^{2+} to Fe^{3+} at pH ~ 10 to 11. Typically, into a 250 mL round-bottom flask were dissolved 0.20 g of $\text{FeCl}_2 \cdot 4\text{H}_2\text{O}$ and 0.27 g of $\text{FeCl}_3 \cdot 6\text{H}_2\text{O}$ in 75 mL of water. After the solution was stirred under nitrogen bubbling for 15 min at 40°C , 6 mL of 1.5 M aqueous ammonium hydroxide solution was added. The pH of the solution was kept at ~ 10 by further addition of 3–4 mL of ammonium hydroxide solution. The color of the solution immediately changed from yellow to black due to the formation of magnetite nanoparticles. The temperature was then raised to 60°C and the solution was stirred for another 30 min. 20 mL of 0.3 M aqueous sodium citrate solution was added and the solution was stirred and heated to 90°C for 30 min to complete the surface coating. The resultant citrate-modified magnetite nanoparticles (MNP-C) were repeatedly precipitated in acetone and washed with deionized water three times, and dried under vacuum to a constant weight.

2) Fabrication of magnetic fluorescent silica nanoparticles (MFSNPs): Silole-APS conjugate (**1**) was prepared by stirring a solution of $6 \mu\text{mol}$ of 1,1-dimethyl-2,5-bis[4-(2-bromoethoxy)phenyl]-3,4-diphenylsilole and $16 \mu\text{mol}$ of APS in $50 \mu\text{L}$ of DMSO overnight. Water was excluded to avoid the possible hydrolysis of the APS to form nanoparticles. The reaction mixture was concentrated under high vacuum and the product was characterized by mass spectroscopy (Figure S1). The magnetic fluorescent silica nanoparticles were fabricated by the Stöber method with some modifications. An ethanol solution (1 mL) of adduct **1** ($6 \mu\text{mol}$) and 0.2 mL of TEOS was first prepared. Into another flask was dispersed 10.0 mg of MNP-C in 32 mL of ethanol with 1.0 mL of ammonium hydroxide and 8.0 mL of distilled water. The mixture was sonicated for 5 min in order to obtain a stable and homogenous magnetic dispersion. The solution containing **1** and TEOS was then added to the magnetic fluid. After stirring at room temperature for 24 h, the mixture was centrifuged and redispersed in ethanol. Such a process was repeated three to four times and the resultant MFSNPs was finally dispersed in water for further applications.

3) Preparation of amino-modified magnetic fluorescent silica nanoparticles (MFSNP- NH_2): MFSNP- NH_2 was synthesized by sol-gel reaction of APS, **1**, and TEOS in the presence of MNP-C in basic ethanol/water mixture. The procedures were the same for the fabrication of MFSNPs. The MFSNP- NH_2 were dispersed in water for the BSA adsorption.

Cell Culture: HeLa cells were cultured in minimum essential medium containing 10% fetal bovine serum and antibiotics ($100 \text{ units mL}^{-1}$ penicillin and $100 \mu\text{g mL}^{-1}$ streptomycin) in a 5% CO_2 humidity incubator at 37°C .

Cell Imaging: HeLa cells were grown overnight on a plasma-treated 25 mm round cover slip mounted onto a 35 mm petri dish with an observation window. The living cells were stained with $250 \mu\text{L}$ of MFSNPs and incubated for 24 h. The cells were imaged under an inverted

fluorescence microscope (Nikon Eclipse TE2000-U); $\text{ex} = 330\text{--}380 \text{ nm}$, diachronic mirror = 400 nm . The images of the cells were captured using a digital CCD camera.

Supporting Information

Supporting Information is available from the Wiley Online Library or from the author.

Acknowledgements

This work was partially supported by the Research Grants Council of Hong Kong (604509, 603008, CUHK1/CRF/08, and HKUST2/CRF/10), the Innovation and Technology Commission (ITP/008/09NP and ITS/168/09), the University Grants Committee of Hong Kong (AoE/P-03/08), the National Science Foundation of China (20974028 and 20634020), and the Ministry of Science & Technology (2009CB623605). B. Z. Tang thanks the supports from the Cao Guangbiao Foundation of the Zhejiang University.

Received: December 7, 2010
Published online: March 22, 2011

- [1] For a review, see: W. J. M. Mulder, A. W. Griffioen, G. J. Strijkers, D. P. Cormode, K. Nicolay, Z. A. Fayad, *Nanomedicine* **2007**, *2*, 307.
- [2] A. Burns, H. Ow, U. Wiesner, *Chem. Soc. Rev.* **2006**, *35*, 1028.
- [3] U. Jeong, X. Teng, Y. Wang, H. Yang, Y. Xia, *Adv. Mater.* **2007**, *19*, 33.
- [4] W. Schärtl, *Adv. Mater.* **2000**, *12*, 1899.
- [5] F. Caruso, *Adv. Mater.* **2001**, *13*, 11.
- [6] H. Kawaguchi, *Prog. Polym. Sci.* **2000**, *25*, 1171.
- [7] D. Dosev, M. Nickkova, R. K. Dumas, S. J. Gee, B. D. Hammock, K. Liu, I. M. Kennedy, *Nanotechnology* **2007**, *18*, 055102.
- [8] J. Gao, B. Zhang, Y. Gao, Y. Pan, X. Zhang, B. Xu, *J. Am. Chem. Soc.* **2007**, *129*, 11928.
- [9] J. Guo, W. Yang, C. Wang, J. He, J. Chen, *Chem. Mater.* **2006**, *18*, 5554.
- [10] S. A. Corr, A. O'Byrne, Y. K. Gun'ko, S. Ghosh, D. F. Brougham, S. Mitchell, Y. Volkov, A. Prina-Mello, *Chem. Commun.* **2006**, 4474.
- [11] Y. S. Lin, S. H. Wu, Y. Hung, Y. H. Chou, C. Chang, M. L. Lin, C. P. Tsai, C. Y. Mou, *Chem. Mater.* **2006**, *18*, 5170.
- [12] F. Bertorelle, C. Wilhelm, J. Roger, F. Gazeau, C. Menager, V. Cabuil, *Langmuir* **2006**, *22*, 5385.
- [13] V. Salgueirino-Maceira, M. A. Correa-Duarte, M. Spasova, L. M. Liz-Marzan, M. Farle, *Adv. Funct. Mater.* **2006**, *16*, 509.
- [14] J. Kim, J. E. Lee, J. Lee, J. H. Yu, B. C. Kim, K. An, Y. Hwang, C. H. Shin, J. G. Park, J. Kim, T. Hyeon, *J. Am. Chem. Soc.* **2006**, *128*, 688.
- [15] S. Santra, R. P. Bagwe, D. Dutta, J. T. Stanley, G. A. Walter, W. Tan, B. M. Moudgil, R. A. Mericle, *Adv. Mater.* **2005**, *17*, 2165.
- [16] G. Wang, E. Song, H. Xie, Z. Zhang, Z. Tian, C. Zuo, D. Pang, D. Wu, Y. Shi, *Chem. Commun.* **2005**, 4276.
- [17] S. K. Mandal, N. Lequeux, B. Rotenberg, M. Tramier, J. Fattaccioli, J. Bibette, B. Dubertret, *Langmuir* **2005**, 4175.
- [18] S. Kim, T. Y. Ohulchanskyy, H. E. Pudavar, R. K. Pandey, P. N. Prasad, *J. Am. Chem. Soc.* **2007**, *129*, 2669.
- [19] H. J. Tracy, J. L. Mullin, W. T. Klooster, J. A. Martin, J. Haug, S. Wallace, I. Rudloe, K. Watts, *Inorg. Chem.* **2005**, *44*, 2003.
- [20] S. J. Toal, D. Magde, W. C. Trogler, *Chem. Commun.* **2005**, 5465.
- [21] B. K. An, S. K. Kwon, S. D. Jung, S. Y. Park, *J. Am. Chem. Soc.* **2002**, *124*, 14410.
- [22] X. J. Zhang, A. S. Shetty, S. A. Jenekhe, *Macromolecules* **1999**, *32*, 7422.

- [23] T. Maka, S. G. Romanov, M. Muller, R. Zentel, C. S. Torres, *Phys. Status Solidi B* **1999**, 215, 307.
- [24] J. R. Lakowicz, J. Malicka, J. Huang, Z. Gryczynski, I. Gryczynski, *Biopolymers* **2004**, 74, 467.
- [25] a) L. Levy, Y. Sahoo, K. S. Kim, E. J. Bergey, P. N. Prasad, *Chem. Mater.* **2002**, 14, 3715; b) S. Setayesh, A. C. Grimsdale, T. Weil, V. Enkelmann, K. Mullen, F. Meghdadi, E. J. W. List, G. Leising, *J. Am. Chem. Soc.* **2001**, 123, 946.
- [26] a) Y. Sahoo, A. Goodarzi, M. T. Swihart, T. Y. Ohulchanskyy, N. Kaur, E. P. Furlani, P. N. Prasad, *J. Phys. Chem. B* **2005**, 109, 3879; b) R. Iqbal, S. C. Moratti, A. B. Holmes, G. Yahioğlu, L. R. Milgrom, F. Cacialli, J. Morgado, R. H. Friend, *J. Mater. Sci. Mater. Electron.* **2000**, 97.
- [27] M. Derfus, W. C. W. Chan, S. N. Bhatia, *Nano Lett.* **2004**, 4, 11.
- [28] J. Yao, D. Larson, H. Vishwasrao, W. Zipfel, W. Webb, *Proc. Natl. Acad. Sci. U.S.A.* **2005**, 102, 14284.
- [29] T. Pellegrino, S. Kudera, T. Liedl, A. Javier, L. Manna, W. Parak, *Small* **2005**, 1, 48.
- [30] H. Ow, D. Larson, M. Srivastava, B. Baird, W. Webb, U. Wiesner, *Nano Lett.* **2005**, 5, 113.
- [31] U. I. Tromsdorf, N. C. Bigall, M. G. Kaul, O. T. Bruns, M. S. Nikolic, B. Mollwitz, R. A. Sperling, R. Reimer, H. Hohenberg, W. J. Parak, S. Forster, U. Beisiegel, G. Adam, H. Weller, *Nano Lett.* **2007**, 7, 2422.
- [32] K. Liu, S. B. Clendenning, L. Friebe, W. Y. Chan, X. B. Zhu, M. R. Freeman, G. C. Yang, C. M. Yip, D. Grozea, Z. H. Lu, I. Manners, *Chem. Mater.* **2006**, 18, 2591.
- [33] C. R. Vestal, Z. J. Zhang, *J. Am. Chem. Soc.* **2003**, 125, 9828.
- [34] F. M. Winnik, A. Morneau, R. F. Ziolo, H. D. H. Stover, W. H. Li, *Langmuir* **1995**, 11, 3660.
- [35] J. Luo, Z. Xie, J. W. Y. Lam, L. Cheng, H. Chen, C. Qiu, H. S. Kwok, X. Zhan, Y. Liu, D. Zhu, B. Z. Tang, B. Z., *Chem. Commun.* **2001**, 1740.
- [36] Y. Hong, J. W. Y. Lam, B. Z. Tang, *Chem. Commun.* **2009**, 4332.
- [37] Z. Zhao, Z. Wang, P. Lu, C. Y. K. Chan, D. Liu, J. W. Y. Lam, H. H. Y. Sung, I. D. Williams, Y. Ma, B. Z. Tang, *Angew. Chem. Int. Ed.* **2009**, 48, 7608.
- [38] Y. Dong, J. W. Y. Lam, A. Qin, Z. Li, J. Sun, Y. Dong, H. H. H. Sung, I. D. Williams, B. Z. Tang, *Chem. Commun.* **2007**, 40.
- [39] H. Tong, Y. Hong, Y. Q. Dong, Y. Ren, M. Häußler, J. W. Y. Lam, K. S. Wong, B. Z. Tang, *J. Phys. Chem. B* **2007**, 111, 2000.
- [40] F. Mahtab, Y. Hong, J. Liu, Y. Yu, J. W. Y. Lam, A. Qin, P. Lu, B. Z. Tang, *Chem. Eur. J.* **2010**, 16, 4266.
- [41] B. Z. Tang, Y. Geng, J. W. Y. Lam, B. Li, X. Jing, X. Wang, F. Wang, A. B. Pakhomov, X. X. Zhang, *Chem. Mater.* **1999**, 11, 1581.
- [42] M. Häußler, R. Zheng, J. W. Y. Lam, H. Tong, H. Dong, B. Z. Tang, *J. Phys. Chem. B* **2004**, 108, 10645.
- [43] M. Häußler, B. Z. Tang, *Adv. Polym. Sci.* **2007**, 209, 1.
- [44] M. Haussler, A. Qin, B. Z. Tang, *Polymer* **2007**, 48, 6181.
- [45] J. Liu, J. W. Y. Lam, B. Z. Tang, *Chem. Rev.* **2009**, 109, 5799.
- [46] T. Matsunaga, R. Sato, S. Kamiya, T. Tanaka, H. Takeyama, *J. Magn. Mater.* **1999**, 194, 126.
- [47] J. I. Taylor, C. D. Hurst, M. J. Davies, N. Sachsinger, I. J. Bruce, *J. Chromatogr. A* **2000**, 890, 159.
- [48] M. T. Reetz, A. Zonta, V. Vijayakrishnan, K. Schimossek, *J. Mol. Catal. A: Chem.* **1998**, 134, 251.
- [49] X. C. Shen, X. Z. Fang, Y. H. Zhou, H. Liang, *Chem. Lett.* **2004**, 33, 1468.
- [50] A. Goodarzi, Y. Sahoo, M. T. Swihart, P. N. Prasad, *Mat. Res. Soc. Symp. Proc.* **2004**, 789, N6.6.1.
- [51] Y. H. Deng, C. C. Wang, J. H. Hu, W. L. Yang, S. K. Fu, *Colloids Surf., A* **2005**, 262, 87.
- [52] a) S. Shouheng, Z. Zeng, B. R. David, R. Simone, M. R. Philip, X. W. Shan, L. Guanxiong, *J. Am. Chem. Soc.* **2004**, 126, 273; b) K. M. Kamruzzaman Selim, Y. S. Ha, S. J. Kim, Y. Chang, T. J. Kim, G. H. Leed, I. K. Kang, *Biomaterials* **2007**, 28, 710.
- [53] Y. Lu, Y. Yin, Z. Yuan Li, Y. Xia, *Nano Lett.* **2002**, 2, 785.
- [54] J. Lee, Y. Lee, J. K. Youn, H. B. Na, T. Yu, H. Kim, S. M. Lee, Y. M. Koo, J. H. Kwak, H. G. Park, H. N. Chang, M. Hwang, J. G. Park, J. Kim, T. Hyeon, *Small* **2008**, 4, 143.
- [55] T. C. Lin, G. Seshadri, J. A. Kelber, *Appl. Surf. Sci.* **1997**, 119, 83.
- [56] R. M. Ottenbrite, J. S. Wall, *J. Am. Ceram. Soc.* **2000**, 83, 3214.
- [57] V. Blaaderen, A. Vrij, *J. Colloid Interf. Sci.* **1993**, 156, 1.
- [58] W. Stöber, A. Fink, J. Bohn, *J. Colloid Interf. Sci.* **1968**, 26, 62.
- [59] S. Sun, H. Zeng, D. B. Robinson, S. Raoux, P. M. Rice, S. X. Wang, G. Li, *J. Am. Chem. Soc.* **2004**, 126, 273.
- [60] J. Yang, J. Lee, J. Kang, C. H. Chung, K. Lee, J. S. Suh, H. G. Yoon, Y. M. Huh, S. Haam, *Nanotechnology* **2008**, 19, 1.
- [61] a) Y. Sahoo, A. Goodarzi, M. T. Swihart, T. Y. Ohulchanskyy, N. Kaur, E. P. Furlani, P. N. Prasad, *J. Phys. Chem. B* **2005**, 109, 3879; b) R. Kumar, I. Roy, T. Y. Ohulchanskyy, L. N. Goswami, A. C. Bonoiu, E. J. Bergey, K. M. Trampusch, A. Maitra, P. N. Prasad, *ACS Nano* **2008**, 2, 449.
- [62] a) J. M. Rosenholm, A. Meinander, E. Peuhu, R. Niemi, J. E. Eriksson, C. Sahlgren, M. Lindén, *ACS Nano* **2009**, 3, 197; b) M. Breunig, S. Bauer, A. Goepferich, *Euro. J. Pharmacol. Biopharmacol.* **2008**, 68, 112.
- [63] X. C. Shen, X. Z. Fang, Y. H. Zhou, H. Liang, *Chem. Lett.* **2004**, 33, 1468.